Chapter 4. Co-delivery of CRAds with MMP-9 Enhances Therapeutic Effect *in Vivo*

4.1 Introduction

In the preceding chapter, CRAds using VEGF or Flt-1 promoters and having Ad3 tropism were evaluated using various mesothelioma cell lines and primary cultures *in vitro*. The logical next challenge is to determine the efficacy in the more complex three-dimensional environment of an *in vivo* tumour.

Many clinical trials of CRAds have been conducted. This approach appears safe, and has some efficacy, but overall the degree of efficacy has been poor. Even with the most permissive tumour lines such as A549, xenografts in immuno-compromised animals are rarely if ever completely eradicated. Strategies to improve viral infectivity by modifying the outer coat protein of the virus have resulted in some therapeutic gains, but in the main these have been modest. Evidence from clinical trials and pre-clinical studies suggests that physical barriers within tumour masses (including necrosis, fibrosis) limit the spread of CRAds. The ideal CRAds would not only have good tropism for target tumour cells, but also have properties that enhance viral spread throughout a tumour mass. The matrix metalloproteinases (MMPs) are a family of proteases, which collectively have the capacity to breakdown all components of the extracellular matrix. Gene delivery for MMP-9 has already been achieved using Ad vectors. Therefore, in the current chapter I decided not only to assess the new vectors as single agents but also to assess the co-delivery of the CRAds along with separate Ads carrying the MMP-9 gene.

I hypothesised that the combination would improve therapeutic efficacy by reducing tumour-associated fibrosis thereby enhancing viral spread through a tumour mass. For this study, I had used the H226 human mesothelioma cell line, as it showed good susceptibility to VEGF and Flt-1 CRAds, and had been reported to readily form tumours in nude mice.

4.2 MMP-9 Protein Expression *in Vitro*

Key to the success of this strategy would be the demonstration that I was able to achieve significant expression of MMP-9 in the context of the replicating viral system. The basic functionality of the AdCMVMMP-9 vector I used here had already established and published by our collaborators in the University of Wales College of Medicine (Cambridge, UK). Thus I compared MMP-9 levels obtained from H226 cells infected either with the vector alone or in combination with the replicative viruses (Adwt, Ad5/3Flt-1E1 or Ad5/3VEGFE1) by Western Blotting. Transgene expression was visualised by using specific antibody human MMP-9. MMP-9 protein expression could be detected in H226 human mesothelioma cells infected with AdCMVMMP-9 alone or combination of Ads and AdCMVMMP-9 (Fig. 4-1).

4.3 Viral Production in Cells Over-expressing MMP-9 *in Vitro*

Measurement of viral production in the presence of MMP-9 expression was used as another test to see if there were any major incompatibilities with the two approaches. From the outset, the fact that I could readily grow batches of high titre AdCMVMMP-9 in 293 cells suggested there ought not to be a problem with MMP-9 expression and viral

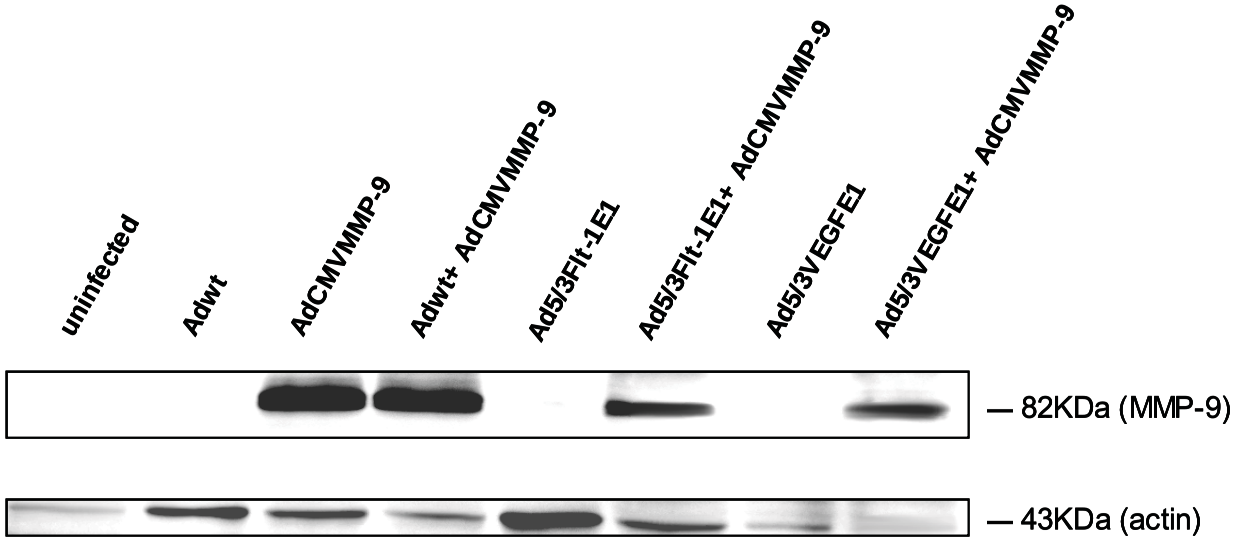

Fig. 4-1 MMP-9 protein expression in H226 human mesothelioma cell line. H226 cells were infected with different viruses:Adwt ± AdCMVMMP-9, Ad5/3Flt-1E1± AdCMVMMP-9 and Ad5/3VEGFE1 ± AdCMVMMP-9 at a dose of 100 MOI. The cells were collected 48 h following infection and lysed with lysis buffer. Western blotting was performed on cell lysates. MMP-9 protein expression could be detected in H226 cells infected with AdCMVMMP-9 alone or combination of Ads and AdCMVMMP-9. The MMP-9 protein size is 82KDa. Actin was used as a house-keeping gene.

replication. Nevertheless studies were conducted in H226 human mesothelioma and A549 lung cancer cell lines. Infections were performed with wild type Ad alone as well as in combination with AdCMVMMP-9. It was felt that Adwt would be generalisable to other replicative Ads in this context. Combination of Adwt and non-replicative control AdCMVLuc used as a negative control for MMP-9 expression. After 24 and 48 h, cells were lysed and supernatant used to quantify viable viral content using the $TCID_{50}$ assay. Measurement of viral production in presence of MMP-9 showed a similar proportional increase in titre from 24 to 48 h whether Adwt was co-infected with AdCMVMMP-9 or with AdCMVLuc, or if used alone. The TCID50 from the H226 cells fell somewhat when either non-replicative Ad was co-infected with the Adwt, but in view of the fact that the drop was similar for the two non-replicative Ads, it was concluded that MMP-9 expression itself was not limiting viral production (Fig. 4-2). There was still an increase in viral output from 24 to 48 hours.

4.4 Co-delivery of CRAds with MMP-9 *in Vivo*

4.4.1 Co-delivery of CRAds with MMP-9 Enhances Therapeutic Effect *in Vivo*

The most important assessment of our attempts to improve the basic efficacy of CRAds using the strategy of enzyme co-expression would be conducted in actual tumour masses *in vivo*. The *in vitro* studies had implied that there were no major incompatibilities with viral production and MMP-9 expression. For these study I used subcutaneous H226 tumour nodules implanted into nude mice. Although growth of H226 cells in nude mice had been previously reported by others, we did encounter some

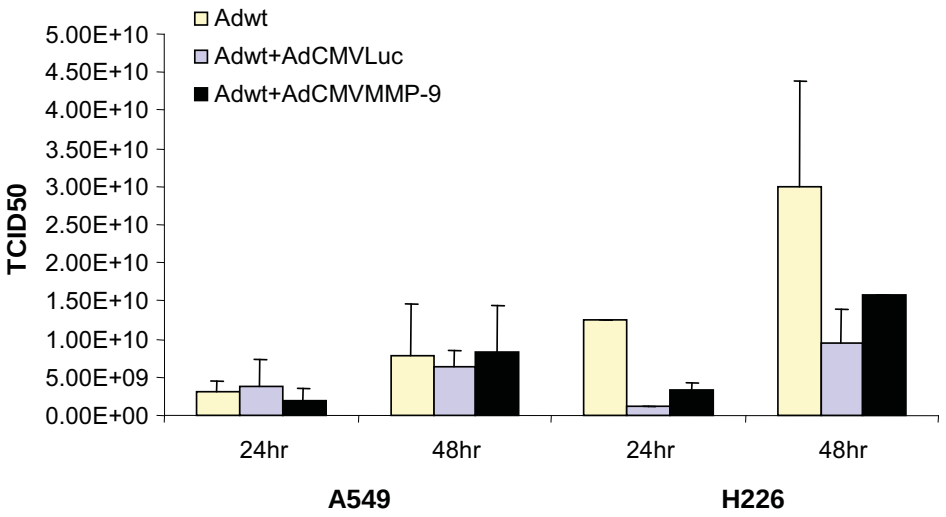

Fig. 4-2 Measurement of viral production in cells infected with AdCMVMMP-9. H226 human mesothelioma and A549 lung cancer cells infected with Adwt alone or in combination with AdMMP-9, combination of Adwt and non-replicative control AdCMVLuc as a negative control. 24 and 48 h post infection, cells were lysed and supernatant used to assess viral content by $TCID_{50}$. Viral production in presence of MMP-9 showed no significant reduction compared to control virus. Data was presented as the mean ± SD of triplicate wells.

problems with a relatively low percentage of inoculated mice developing tumours. Discussions with colleagues in the field revealed similar problems but this was not something apparent from the published literature. In an effort to improve on the percentage of animals developing assessable tumours, a new line was established from animals that developed tumours from the initial inoculation. We designated this line H226T, and have since found that virtually 100% of animals inoculated with these selected cells develop tumours. No changes to susceptibility *in vitro* to viral agents were detected.

Once the initial difficulties with the model system were overcome, and tumour growth was more reliable, studies could proceed. After inoculation, when tumours had reached 50 mm^3 in size, they were injected with various viruses: Ad5/3VEGFE1, Ad5/3Flt-1E1, AdCMVMMP-9 in combination with either AdCMVMMP-9 or control virus AdCMVLuc. The choice of CRAds used in this evaluation was based on the efficacy shown in the initial *in vitro* analyses. A control group of animals received injections of saline. Eight mice per group were used. All control mice were sacrificed before treatment groups. CRAds and AdCMVMMP-9 in combination with either AdCMVMMP-9 or control virus inhibited tumour growth (Figure 4.3). The effect of the CRAds compared to the non-replicative MMP-9 plus AdCMVLuc combination was rather disappointing however, despite the earlier good killing effect seen *in vitro*. Combination of CRAds driven by tumour-specific promoters VEGF and Flt-1 with AdCMVMMP-9 resulted the greatest growth inhibition compared to the two viruses combined with control virus AdCMVLuc. Percent survival rates in Figure 4-4 indicated all treatment groups improved the survival compared to PBS group. Co-delivery of

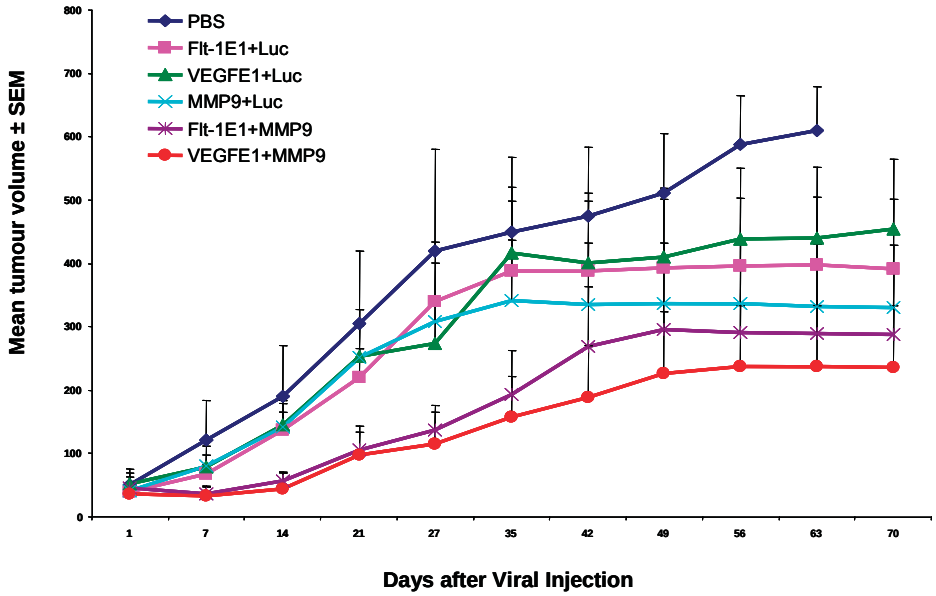

Fig. 4-3 Tumour size of co-expression MMP-9 with CRAds *in vivo*. Mice were injected with H226 tumour and then received Ad5/3VEGFE1, Ad5/3Flt-1E1, AdCMVMMP-9 in combination with either AdCMVMMP-9 or AdCMVLuc. Control group received injection of saline. CRAds and AdMMP-9 in combination with either AdMMP-9 or control virus delayed tumour growth. Combination of Ad5/3VEGFE1 or Ad5/3Flt-1E1 with AdCMVMMP-9 achieved the greatest therapeutic effect compared to CRAds VEGF or Flt-1 combined with control virus. Data was presented as mean tumour volume ± SEM (n=8 mice per group).

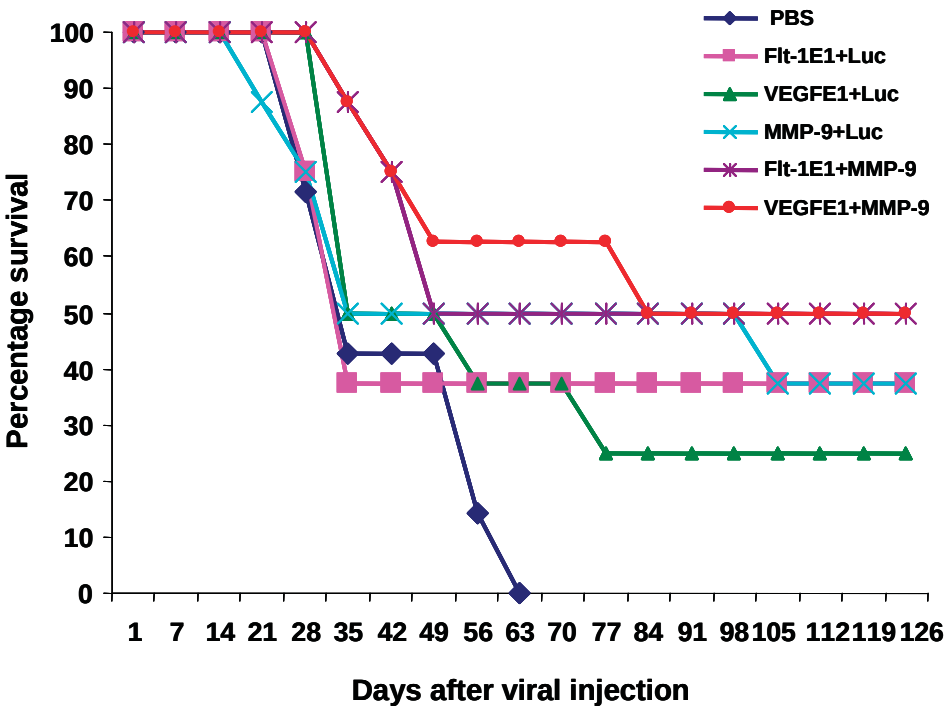

Fig. 4-4 Survival of co-expression MMP-9 with CRAds *in vivo*. All treatment groups improved the survival compared to PBS group. Co-delivery of Ad5/3Flt-1E1 or MMP-9 with control virus showed the same survival rates, and slightly improved survival than Ad5/3VEGFE1 combined with control virus. Combination of CRAds and AdCMVMMP-9 resulted the greatest survival in all groups.

Ad5/3Flt-1E1 or MMP-9 with control virus showed the same survival rates, and slightly improved survival than Ad5/3VEGFE1 combined with control virus. Combination of CRAds and AdCMVMMP-9 resulted the greatest survival in all groups. There were still 4 mice surviving in each group of combined Ad5/3VEGFE1 or Ad5/3Flt-1E1 with AdCMVMMP-9 at the end of the experiment. However, no statistically significant difference was detected in survival, but there was a statistically significant effect on tumour size in the early part of the experiment (at least to day 21). The statistical analysis was greatly aided by the University of Adelaide Statistics core facility and is discussed below:

Statistical analysis – using data from mice alive at day 21

As a sensitivity analysis, the above analyses only using those mice that were still alive at day 21 (i.e. excluding the two mice that had been sacrificed). Results are shown below.

Source	DF	Sum of Squares	Mean Square	F Value	P-value
Model	5	155054.9265	31010.9853	2.49	0.0472
Error	39	485082.9889	12438.0254		
Corrected Total	44	640137.9154			

After excluding mice that had been sacrificed by day 21, there was evidence for a difference in changes in tumour volumes across the six groups ($p = 0.0472$).

Group	Mean change	Standard Error
MMP9+Luc	164.46	42.153
PBS	172.72	45.530
VEGFE1+Luc	201.42	39.430
VEGFE1+MMP9	61.14	39.430
Flt-1E1+Luc	179.54	39.430
Flt-1E1+MMP9	59.19	39.430

Given that there was an overall difference between the six treatment groups, we have calculated the p-values of pairwise comparisons below.

P-values of post-hoc comparisons						
i/j	1	2	3	4	5	6
1		0.8947	0.5257	0.0812	0.7953	0.0759
2	0.8947		0.6364	0.0715	0.9105	0.0669
3	0.5257	0.6364		**0.0161**	0.6968	**0.0148**
4	0.0812	0.0715	**0.0161**		**0.0401**	0.9723
5	0.7953	0.9105	0.6968	**0.0401**		**0.0371**
6	0.0759	0.0669	**0.0148**	0.9723	**0.0371**	

1 = MMP9+Luc, 2 = PBS, 3 = VEGFE1+Luc, 4 = VEGFE1+MMP9, 5 = Flt-1E1+Luc, 6 = Flt-1E1+MMP9

The table shows that changes (increases) in tumour volumes between baseline and day 21 were lower in the VEGFE1+MMP9 group compared to the VEGFE1+Luc and Flt-1E1+Luc groups ($p = 0.0161$ and $p = 0.0401$ respectively). Similarly, increases in tumour volumes between baseline and day 21 were lower in the Flt-1E1+MMP9 group

compared to the VEGFE1+Luc and Flt-1E1+Luc groups ($p = 0.0148$ and $p = 0.0371$ respectively).

4.4.2 Histologic Analysis of Metastasis

Many studies have shown that enhanced production of matrix metalloproteinase (MMP) family contributes to tumour invasion, metastasis, and angiogenesis (Rao et al., 2005). In order to analyse metastasis, the tissues (tumour, lung and liver) from each mouse were removed and fixed in 10% buffered-formalin, and then H&E staining were performed. The histologic analysis (H&E staining) of metastatic foci among the lungs and livers from the mice. Analysis of the metastases in serial lung and liver sections was done under light microscopy. The sections were screened and evaluated by a pathologist (Prof Vernon-Roberts, IMVS) blinded to treatment condition. H226 tumours were treated with 6 groups: Ad5/3VEGFE1, Ad5/3Flt-1E1, AdCMVMMP-9 in combination with either AdCMVMMP-9 or control virus AdCMVLuc, or PBS control group. However, no lung and liver metastases were observed until the end of the experiments in treated or untreated mice.

4.4.3 Immunohistochemical Analysis of Adenovirus Localisation

Adenovirus localisation was also detected by immunohistochemistry. H226 tumours were harvested at time of sacrifice (Day 18 to Day 126 after treatment). The tissues from each mouse were removed, and fixed in 10% buffered-formalin. The tissues were processed into paraffin blocks after overnight fixation and sections cut at 5μm. Immunohistochemical staining of adenovirus was performed on paraffin embedded

specimens. Immunohistochemical staining results (Fig.4-5) showed positive virus distribution within Ad injected tumours. There is no positive staining in PBS control group. Only few positive cells were found in the tumours injected with AdCMVMMP-9 in combination with AdCMVLuc. Adenoviral staining was more readily seen in the tumours that had been injected with replicative Ads, but even here the distribution was fairly limited. This likely reflects the time of sacrifice and tumour harvest which was determined by the large size of the tumour.

4.5 Discussion

My aim was to evaluate the therapeutic effect of tumour-specific CRAds alone and in combination with AdMMP-9 in an *in vivo* model of subcutaneous mesothelioma tumour nodules in nude mice. In the first instance, it was important to determine MMP-9 protein expression and viral production of tumour-specific CRAds alone and in combination with AdMMP-9 *in vitro*. Western blotting result showed the MMP-9 protein expression could be detected in H226 cells infected with AdCMVMMP-9 alone or in combination of Adwt, Ad5/3Flt-1E1, or Ad5/3VEGFE1. In order to reduce variability related to CRAds driven by tumour-specific promoters VEGF and Flt-1, I investigated significant expression of MMP-9 in the context of the replicating viral system by using wild type Ad. Viral production in presence of MMP-9 showed no significant reduction compared to control virus. I do not necessarily expect MMP-9 to improve cell killing *in vitro* (fibrosis etc being more relevant to tumour masses *in vivo*). These studies evaluated the dynamic interaction between these two viruses.

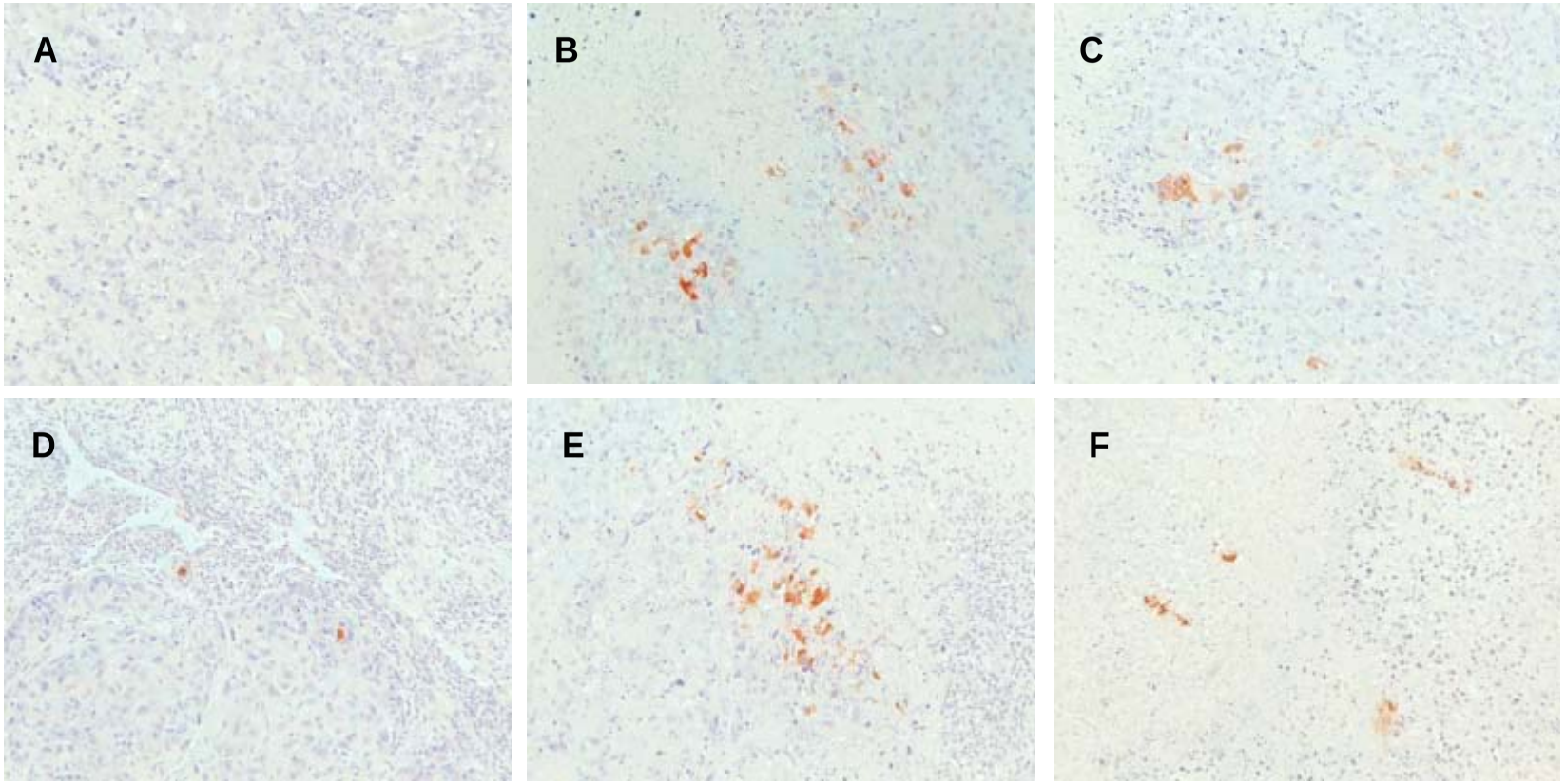

Fig. 4-5 Adenovirus localisation was detected by immunohistochemistry. H226 tumours harvested at time of sacrifice . The tumours were sectioned and stained for adenovirus distribution on paraffin embedded specimens . A: PBS; B: Ad5/3Flt-1E1+AdCMVLuc; C: Ad5/3VEGFE1+AdCMVLuc; D: AdCMVMMP-9+AdCMVLuc; E: Ad5/3Flt-1E1+ AdCMVMMP-9; F: Ad5/3VEGFE1+ AdCMVMMP-9. Immunohistochemical staining showed virus within Ad injected tumours (brown staining, x100 magnification).

I co-delivered CRAds driven by tumour-specific promoters VEGF and Flt-1 with MMP-9 *in vivo*. In this study, mice were treated with 6 groups: PBS, Ad5/3Flt-1E1+AdCMVLuc, Ad5/3VEGFE1+AdCMVLuc, AdCMVMMP-9+AdCMVLuc, Ad5/3Flt-1E1+AdCMVMMP-9, and Ad5/3VEGFE1+AdCMVMMP-9. According to the cell killing results showed in Chapter 3, Ad5/3 demonstrated higher cell killing effect than Ad5 in the H226 cell line. Thus I employed Ad5/3 to assess the impact of co-delivery of CRAds with MMP-9 *in vivo*. I found that combination of CRAds driven by tumour-specific promoters VEGF and Flt-1 with AdCMVMMP-9 resulted the greatest growth inhibition, and that viral therapy *per se* was associated with greater survival than treatment with PBS. Further studies are needed to confirm whether MMP-9 improves therapeutic efficacy due to reducing tumour-associated fibrosis thereby enhancing viral spread through a tumour mass. A likely major limitation of the current study is the fact that the AdCMVMMP-9 vector used here was not itself replication competent. I had postulated that the co-administration with a replication competent vector would provide transcomplementation of E1 and allow a degree of AdCMVMMP-9 replication to occur. However, my inability to detect any MMP-9 expression in the tumours at the time of harvest (despite seeing some positive signal for Ad per se) suggests that this was simply not efficient enough, if it occurred at all. Future evaluations of this system could consider repeated injections of AdCMVMMP-9 or construction of an armed CRAd, containing MMP-9 in the genome (eg in the E3 region). The fact that virus could still be detected in tumours at time of sacrifice (in some cases several weeks after initial injection) is consistent with previous reports. It again highlights the problem of the virus losing its ability to spread and suggests that later injections with MMP-9 could possibly allow for further dispersal of the replicative Ad. These opinions were considered but on balance it was felt that an ultimately more useful clinical approach (and one better to

focus on in the time available) would be to combine viral and immunotherapy, as I discuss in Chapter 5. Of course the approaches are not mutually exclusive and immunotherapy could combine with an optimised CRAd-MMP-9 system in theory.

It has been shown in some settings that higher levels of MMP expression are associated with greater risk of metastases and this would certainly be a concern and need careful safety evaluation if such a strategy were to advance further. This was always a potential concern with the MMP-9 approach. In my study however, I found no lung and liver metastases were observed by H&E staining at least by the end of the experiments in treated or untreated control mice. It suggested that H226 (human mesothelioma cell line) did not form metastases in the nude mice that received s.c inoculation, and expression of MMP-9 in the context of the replicating viral system did not cause lung and liver metastases.

In summary the combination of CRAds with MMP-9 expression did not appear unsafe within the limits of the study, and there was increased efficacy at early time points but further optimisation is required.

Chapter 5. Combination of Viral Therapy and Immunotherapy Enhances the Therapeutic Effect in an Immunocompetent Murine Mesothelioma Model

5.1 Introduction

Stimulation of anti-tumour immunity has long been a subject of intense research, and has the potential major benefit of eliminating both primary and metastatic disease. Cancer therapy approaches based on efforts to stimulate the immune system have received a great deal of attention for a number of years, and many have incorporated gene delivery aspects (either through DNA vaccines or cytokines gene delivery for example)(Robinson et al., 1998; Rosenberg 2001). In general however, results of immunotherapy alone have been disappointing, and certainly the efficacy of these approaches is reduced when tumour burden is high (Odaka et al., 2001). It has been established that responses to immunotherapy can be enhanced by initial debulking of tumours, or by the induction of apoptosis in tumour cells (Nowak et al., 2003). Given that viral therapy is associated with the induction of an inflammatory response, combining viral therapy with immunotherapy could capitalise upon viral induced de-bulking and enhanced influx of effector cells. To date, appropriate model systems have not been available to fully explore the potential of the combined therapy, because human adenovirus typically replicates very poorly in murine cells, thus previous work has relied on human xenografts in immuno-deficient mice, precluding evaluation of combined therapy.

In my study, I identified an immuno-competent murine model of mesothelioma, which is permissive for adenoviral replication. In this model, I determined the feasibility of combining replication competent viral therapy and immunotherapy, in the hopes that this combination would offer greater therapeutic benefit than either treatment alone.

5.2 Establish Adenovirus-Susceptible, Immuno-competent Murine Model for Mesothelioma

5.2.1 Luciferase Gene Expression in Murine Mesothelioma Cells

Human adenoviruses typically do not replicate in mouse cells, due to an incompletely understood block in transcription of late viral genes. For this reason CRAds have not been extensively evaluated in immuno-competent models, but rather in human xenograft models in nude mice. Our collaborators in WA developed a number of unique mouse mesothelioma lines (eg. AE17, AE1, AE1750, AB1, mm6). I assessed the CMV, VEGF and Flt-1 promoter activities in the Ad vectors containing the luciferase gene as a reporter in mouse mesothelioma cell lines AE17, AE1, AE1750, AB1, mm6 and Lung cancer cell line A549. The cells were infected at an MOI of 100 and luciferase activity was measured 48 h later. Figure 5-1 showed luciferase gene expression in murine mesothelioma and adenocarinoma cells. Compared to A549 cell line, human Ad demonstrated low luciferase activity in all mouse mesothelioma cell lines even when the cells were infected at high dose of viruses. However, the AE17 and AE1 cells were noticeably more susceptible than the other mouse lines when using the Ad5CMVLuc vector. Ad5/3 tropism VEGF-luciferase vector demonstrated higher promoter activity than Ad5 tropism VEGF-luciferase vector in A549 adenocarinoma cells. However, Ad5

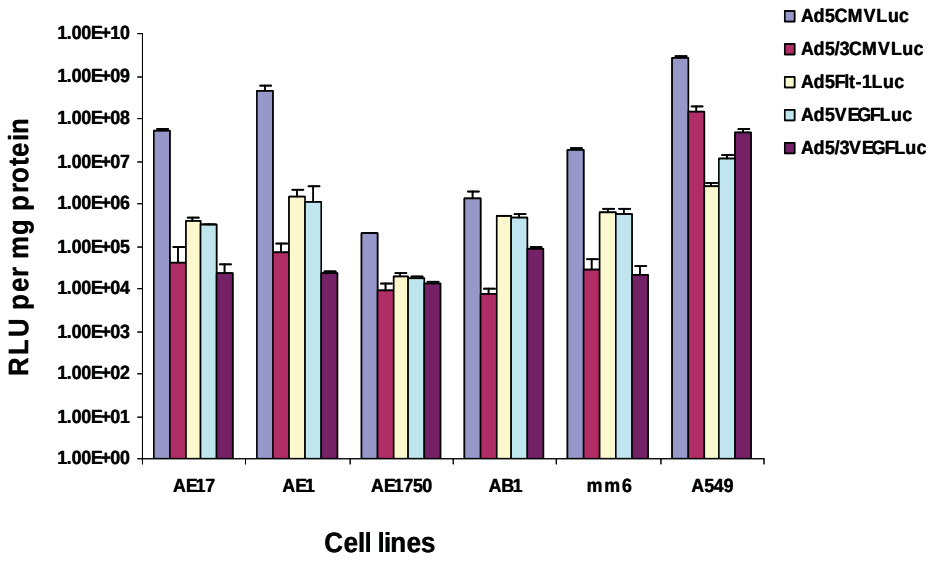

Fig. 5-1 Luciferase expression from Ad vectors in mouse mesothelioma cell lines. Lung cancer cell line A549 and mouse mesothelioma cell lines AE17, AE1, AE1750, AB1 and mm6 were infected with different viruses at an MOI of 100 and luciferase activity was measured 48 h later. Compared to A549 cell line, human Ad demonstrated low luciferase activity in all mouse mesothelioma cell lines. Ad5 demonstrated higher luciferase activity than Ad5/3 in murine cells. Data were presented as the mean ± SD of triplicate wells.

demonstrated higher luciferase activity than Ad5/3 in murine cells, which is consistent with the fact that murine cells do not express CD46.

5.2.2 Cell-killing Efficacy of Human Ads in Murine Mesothelioma Cells

I also tested all available lines (eg. AE17, AE1, AE1750, AB1, mm6) for susceptibility to killing with adenovirus. To avoid potentially confounding the analysis by using CRAds in which E1 is controlled by human promoters, I first screened mouse cells using wild type adenovirus and a CRAd (Δ24RGD) in which E1 is mutated but not dependent on the activity of a human promoter. AdΔ24RGD also has the advantage that it has tropism-expansion by virtue of the additional RGD motif that enables infection via integrin binding and is thus not reliant on CAR. I infected the cells with non-replicative control AdCMVLuc and replicative viruses, Adwt and AdΔ24RGD, and then stained the attached cells with crystal violet 96 h post infection and counted viable cells by measuring OD_{570}. I found 2 lines (AE17 and AE1) that were highly susceptible to killing with replicative Ad (Fig.5-2). I also assessed cell-killing capacity of Adwt and AdΔ24RGD in AE17 and AE1 cell lines by dose-dependence and time-course assays. AE17 and AE1 cells were infected with AdCMVLuc, Adwt and AdΔ24RGD at pfu per cell of 100 down to 0, and the cell-killing effect was obvious at 50 and 100 pfu/cell through 96 h after infection. The cell-killing effect was dose-dependent with maximum effect seen at the highest dose used, 100 pfu/cell (Fig.5-3). The result of time-course assay revealed that the cell-killing effect in the two lines peak at 96 h after the cells infected at a dose of 100 pfu/cell (Fig.5-4). The two lines most susceptible to cell killing

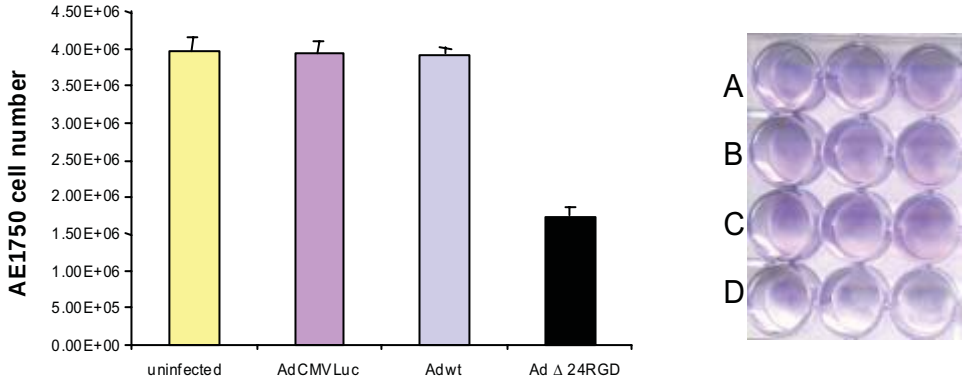
AE1750 cell number
4.50E+06
4.00E+06
3.50E+06
3.00E+06
2.50E+06
2.00E+06
1.50E+06
1.00E+06
5.00E+05
0.00E+00
uninfected
AdCMVLuc
Adwt
Ad Δ 24RGD
A
B
C
D

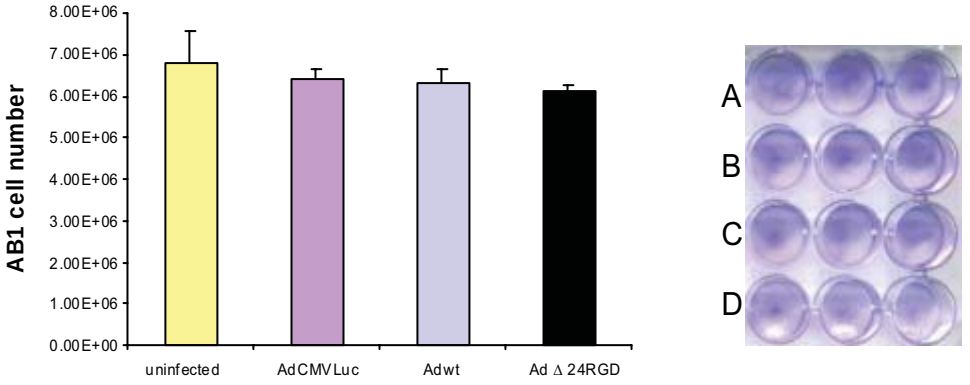
AB1 cell number
8.00E+06
7.00E+06
6.00E+06
5.00E+06
4.00E+06
3.00E+06
2.00E+06
1.00E+06
0.00E+00
uninfected
AdCMVLuc
Adwt
Ad Δ 24RGD
A
B
C
D

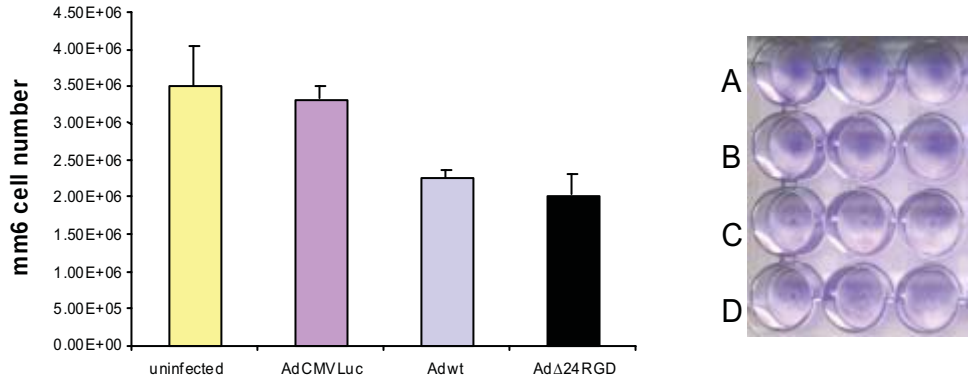
mm6 cell number
4.50E+06
4.00E+06
3.50E+06
3.00E+06
2.50E+06
2.00E+06
1.50E+06
1.00E+06
5.00E+05
0.00E+00
uninfected
AdCMVLuc
Adwt
AdΔ24RGD
A
B
C
D

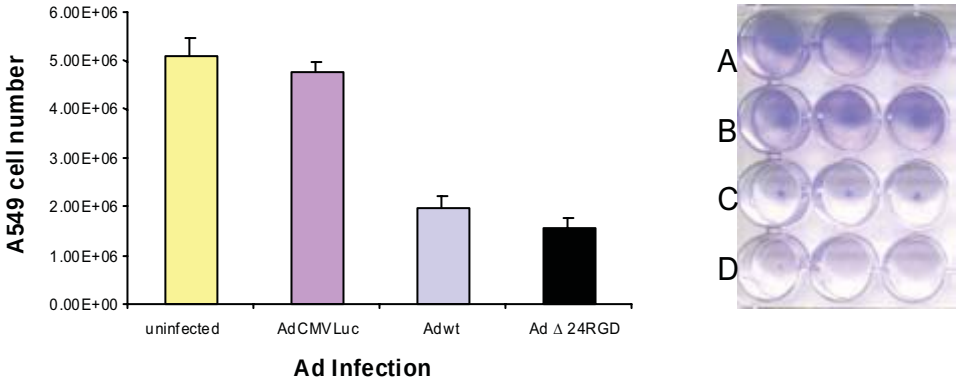
A549 cell number
6.00E+06
5.00E+06
4.00E+06
3.00E+06
2.00E+06
1.00E+06
0.00E+00
uninfected
AdCMVLuc
Adwt
Ad Δ 24RGD
Ad Infection
A
B
C
D

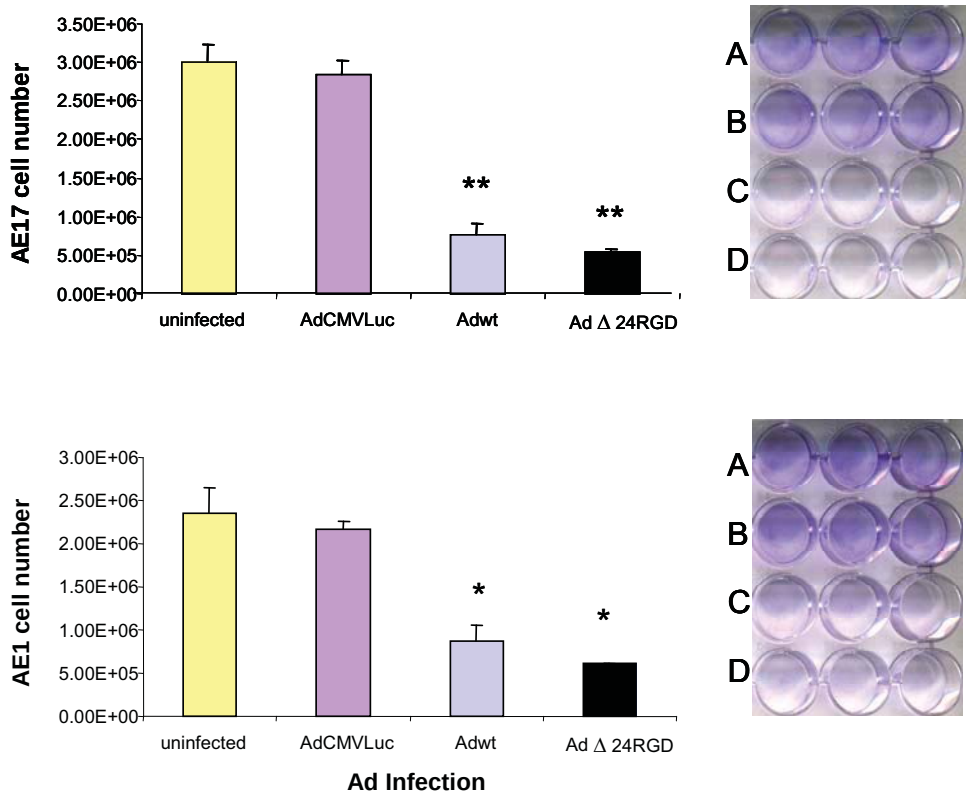

Fig. 5-2 Oncolytic potency of wild type Ad and a CRAd Δ24RGD in mouse mesothelioma cell lines. Cells were infected with different viruses: A.uninfected B.AdCMVLuc C. Adwt D. AdΔ24RGD. The attached cells were stained with crystal violet 96 h after infection and cell viability was determined by measuring OD570nm. AE1 and AE17 cell lines are quite sensitive to killing with wild type Ad and infectivity-enhanced AdΔ24RGD, comparable to the known permissive A549 lung cancer line. Data were presented as the mean ± SD of triplicate wells. *P < 0.05 **P < 0.01 compared with uninfected cells or control virus.

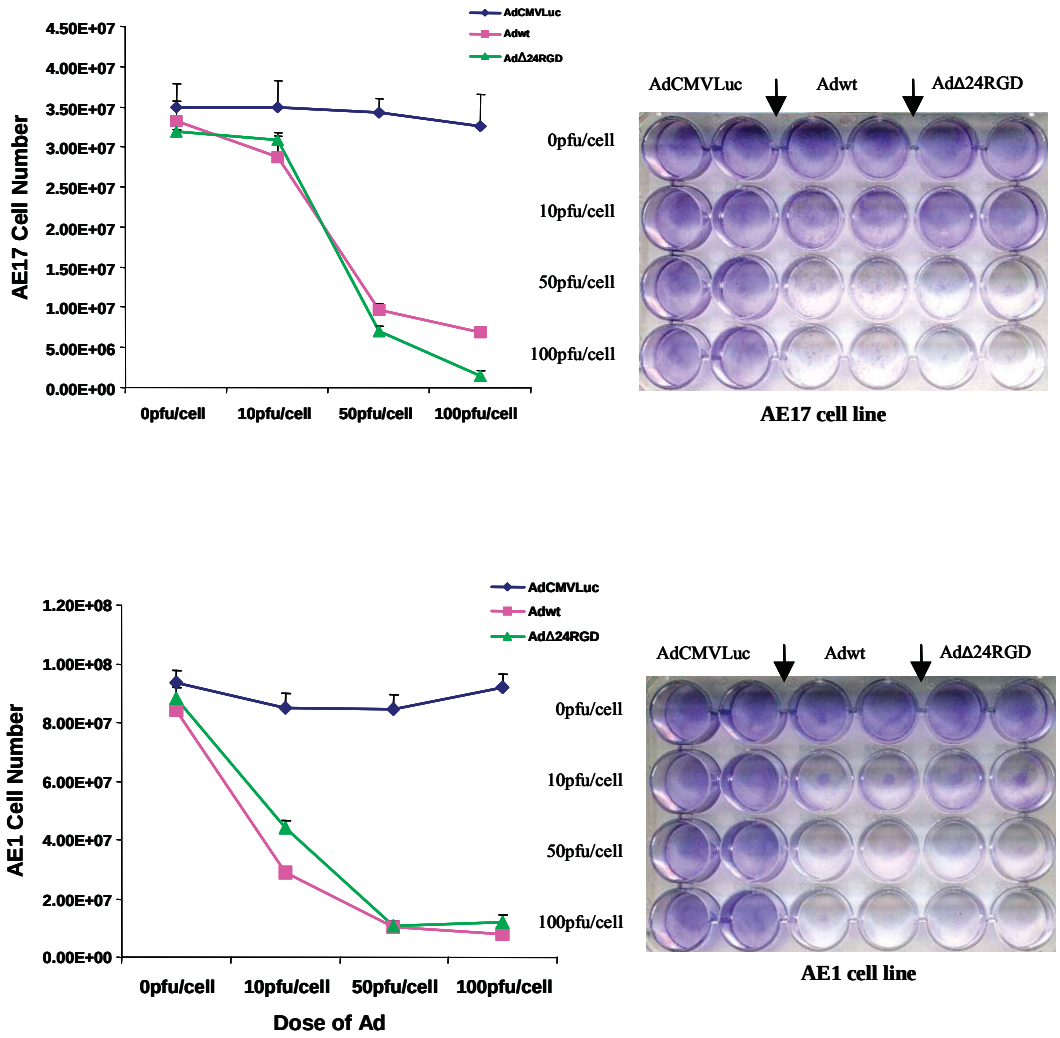

Fig. 5-3 Oncolytic potency of wild-type Ad and a CRAd Δ24RGD in mouse mesothelioma cell lines (dose-dependence assay). AE17 and AE1 cells were infected with different viruses:AdCMVLuc, Adwt and AdΔ24RGD (duplicate) at pfu per cell of 100 down to 0. The attached cells were stained with crystal violet 96 h post infection and cell viability was determined by measuring OD570nm. AE1 and AE17 cell lines that supported the highest cell-killing effect at 100 pfu/cell through 96 h post infection. Data were presented as the mean ± SD of triplicate wells.

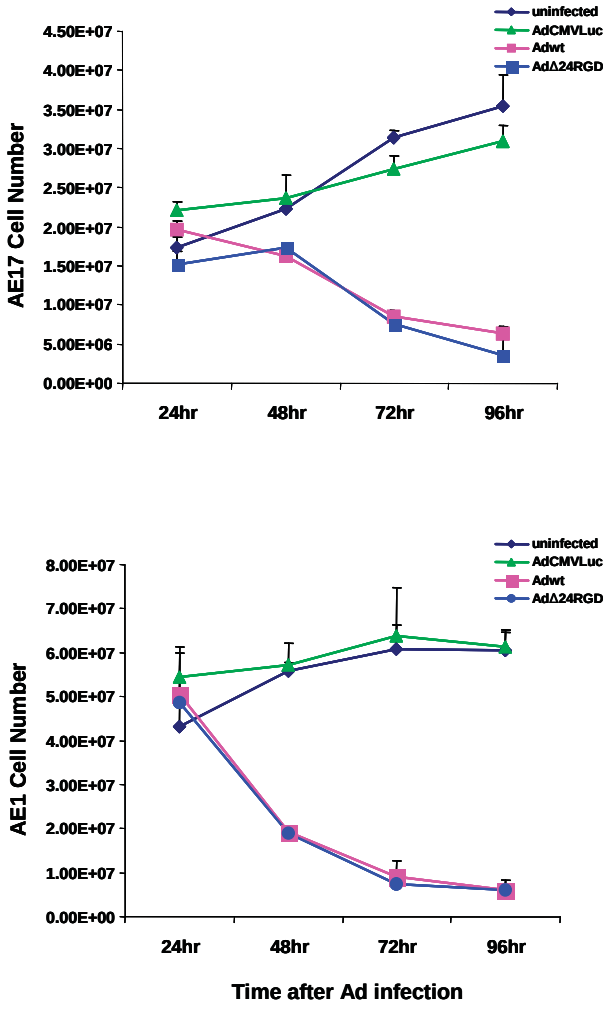

Fig. 5-4 Oncolytic potency of wild-type Ad and a CRAd Δ24RGD in mouse mesothelioma cell lines (time-course assay). AE17 and AE1 cells were infected with different viruses:AdCMVLuc, Adwt and AdΔ24RGD at a dose of 100 MOI. The attached cells were stained with crystal violet in the panel at 24,48,72,96 h following infection and cell viability was determined by measuring OD570nm. The cell-killing effect in the two cell lines peaked at 96 h post infection. Data were presented as the mean ± SD of triplicate wells.

were also the two that had been most susceptible to transduction with the AdCMVLuc vector.

5.2.3 Viral Replication of Human Ads in Murine Mesothelioma Cells

In addition to cell killing I wished to confirm that I was genuinely seeing an increase in viable viral output after infection, rather than a killing effect related to toxicity alone. I chose to use titre assays as the most rigorous assessment, rather than quantification of viral DNA, because DNA replication could occur independently of viable virus output. My studies confirmed an increase in viral titre after infection. AE17 and AE1 cells were infected with AdCMVLuc, Adwt and AdΔ24RGD. I collected the cells after 0 and 24 h infection, and then performed $TCID_{50}$ on 293 cells. Viral replication of Adwt and AdΔ24RGD can be detected 24 h post infection in AE17 and AE1 cells, comparable to non-replicative virus AdCMVLuc (Fig.5-5). Significant differences were found between different time points. The result revealed that human adenoviruses could replicate in murine mesothelioma cell lines. To further validate the assay and to put these results in context I performed the same analysis using the A549 human lung cancer cells that are well known to be highly permissive for Ad replication. An increase in Ad titre was seen as for the murine cells, although the magnitude of increase was much greater in the human cells (Fig.5-5).

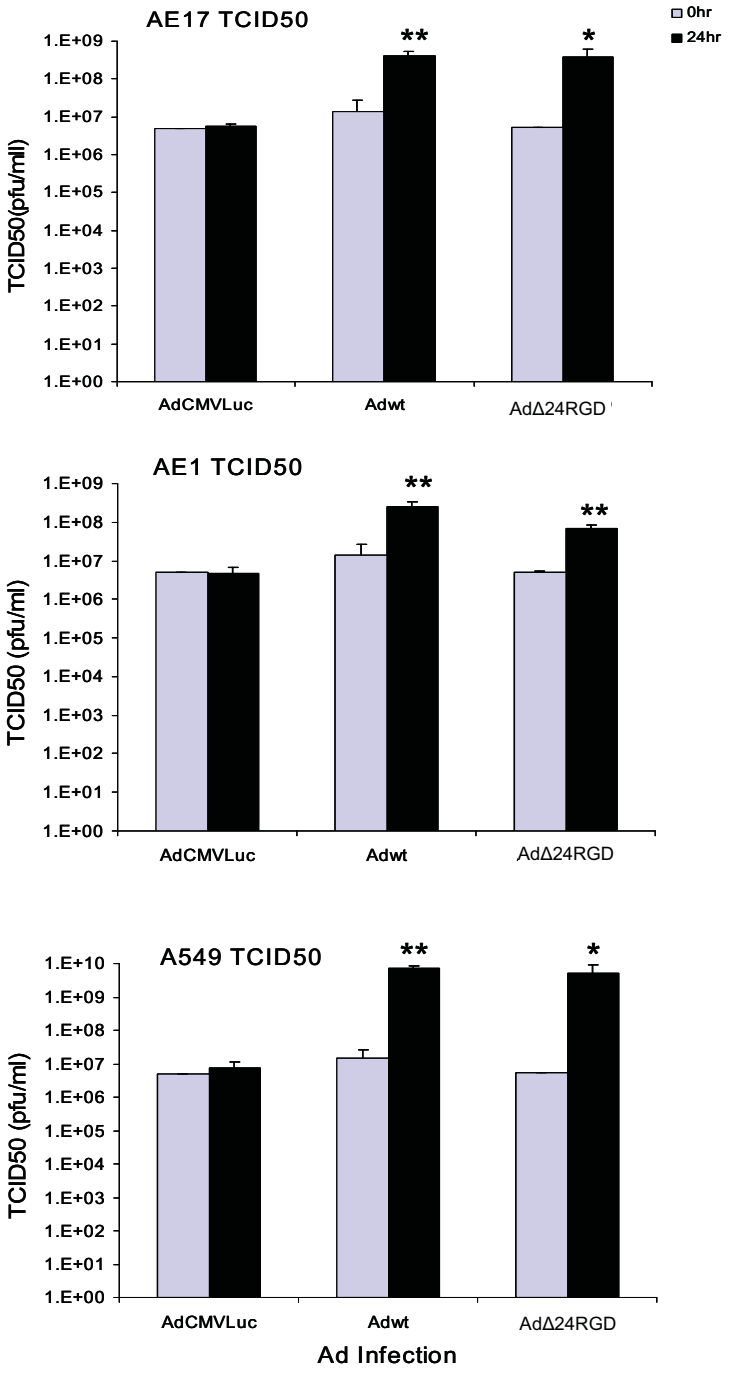

Fig. 5-5 Viral replication of human adenovirus in murine mesothelioma cells and A549 human lung cancer cells. AE17, AE1 and A549 cells were infected with AdCMVLuc, Adwt and AdΔ24RGD at a dose of 100 MOI. Cells were collected after 0 and 24 h infection, and then performed $TCID_{50}$ on 293 cells. Data were presented as the mean ± SD of triplicate wells. Significant difference between different time points * $p < 0.05$; ** $p<0.01$.

5.2.4 Inhibition of Tumour Growth of Human Ads in Murine Model

My initial results *in vivo* showed reduction in tumour growth after viral injection with wild type Ad. AE17 and AE1 cells were implanted subcutaneously in C57 black6 mice. Only AE17 cells formed tumours in mice. Tumours were injected with PBS, AdCMVLuc or Adwt on day 17 after AE17 cells implantation (10 mice per group). Shown in Fig.5-6 is *in vivo* result representative of tumour volume change using a single viral injection. AE17 cells implanted in C57 black6 mice formed rapidly growing tumours, but growth is inhibited by a single injection of replicative Ad compared to saline and non-replicative control Ad *in vivo*. Adenovirus localisation was also detected by immunohistochemistry. Tumours were harvested at time of sacrifice (Day 26 after cell implantation). The tissues from each mouse were removed, and fixed in 10% buffered-formalin. The tissues were processed into paraffin blocks after overnight fixation and sections cut at 5μm. Immunohistochemical staining of adenovirus was performed on paraffin embedded specimens. Immunohistochemical staining results (Fig.5-7) showed positive virus distribution within tumours injected with Adwt. Taken together with the *in vitro* studies, these findings indicate that an immuno-competent murine model of mesothelioma in which the tumours are susceptible to adenoviral replication has been established.

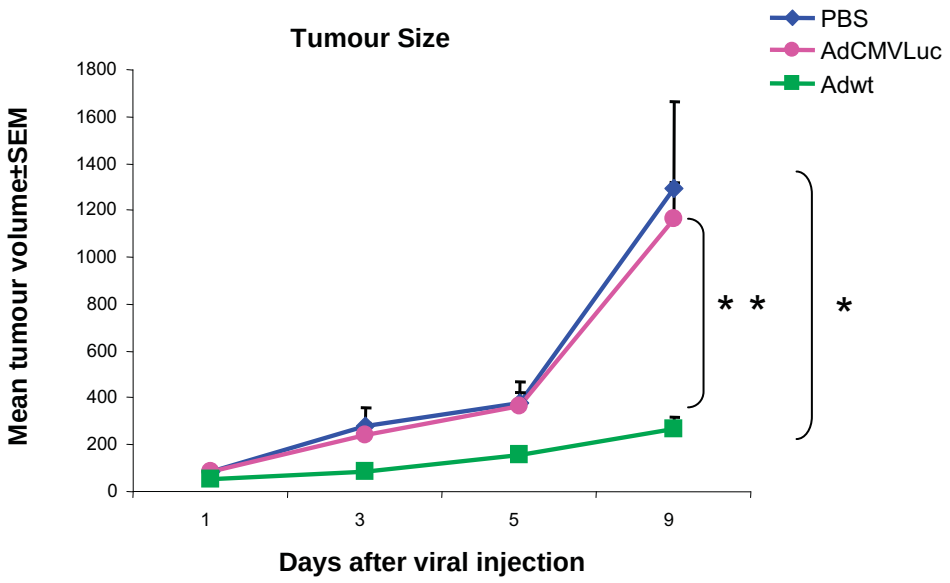

Fig. 5-6 Delivery of Adwt to AE17 tumours causes a size reduction. C57 black6 mice were injected subcutaneously with $5x10^5$ AE17 cells, and tumours were injected with PBS, AdCMVLuc or Adwt. AE17 cells implanted in C57 black6 mice form rapidly growing tumours, but growth is inhibited by a single injection of replicative Ad compared to saline and non-replicative control Ad *in vivo*. Data was presented as mean ± SEM. * $p < 0.05$ Adwt vs PBS; ** $p<0.01$ Adwt vs AdCMVLuc (n = 10 mice per group).

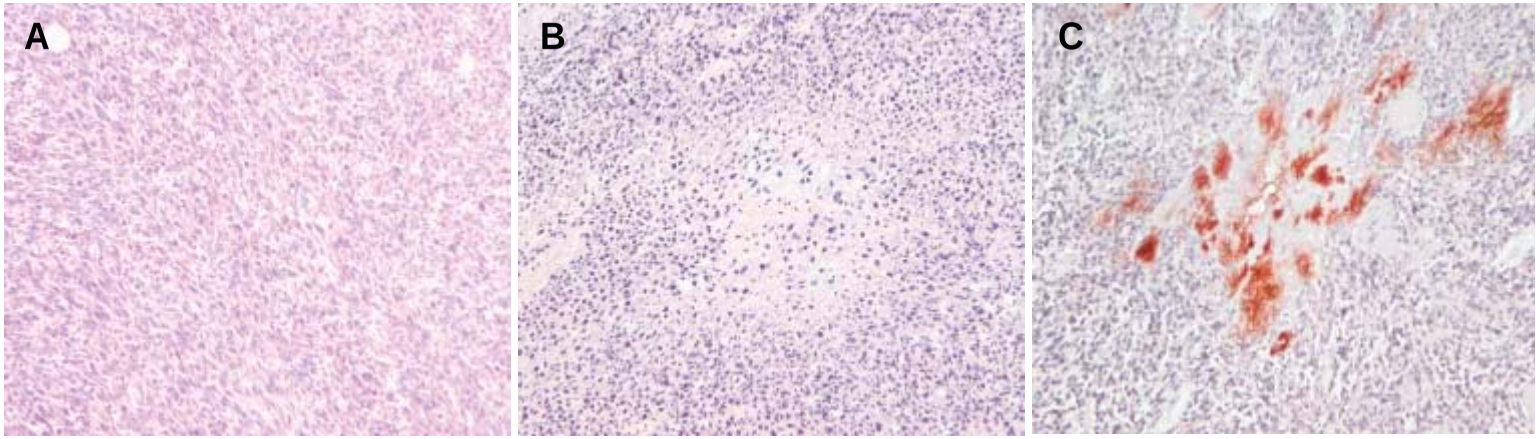

Fig. 5-7 Adenovirus localisation was detected by immunohistochemistry. AE17 tumours harvested at time of sacrifice (Day 26 after AE17 implantation). The tumours were sectioned and stained for adenovirus distribution on paraffin embedded specimens. A: PBS; B: AdCMVLuc; C: Adwt. Immunohistochemical staining showed virus within Adwt injected tumours (brown staining, x100 magnification).

5.3 Combination of Viral Therapy and Immunotherapy in Immuno-competent Murine Mesothelioma Model

5.3.1 CD40 and FGK45

Stimulation of anti-tumour immunity may eliminate both primary and metastatic disease. Combining viral therapy with immunotherapy could capitalise upon viral induced de-bulking and enhanced influx of effector cells. CD40 is a member of the tumour necrosis factor receptor superfamily, which was first identified on bladder carcinoma cells and later on normal and malignant B cells (Paulie et al., 1985). It has been found that CD40 is expressed on dendritic cells, monocytes, epithelial cells, carcinomas of the lung, colon and breast and leukaemia. CD40 activation stimulates effector immune responses. The activating anti-CD40 antibody FGK45 augments CD4 T cells in priming dendritic cells to activate CD8 cytotoxic T cells. The combination of viral-induced tumour debulking and concurrent stimulation of anti-tumour immune responses by FGK45 is thus an attractive proposition.

5.3.2 FGK45 Caused No Toxicity to AE17 cells *in Vitro*

In order to test whether FGK45 causes toxicity to AE17 cells, AE17 cells were infected with AdCMVLuc or Adwt at pfu per cell of 100 (uninfected cells as control). 30ug/ml of FGK45 was added 24 h post infection. The attached cells were stained with crystal violet 144 h post infection and cell viability was determined by measuring OD570nm. No toxicities have been seen in the AE17 cells infected with FGK45 alone or combined

with viruses and there is an indication that FGK45 caused no toxicity to AE17 cells *in vitro* (Fig.5-8).

5.3.3 Combination of Adenovirus and FGK45 Resulted in Greatest Survival

Several efforts were made to optimise the model system. The major issues that needed to be addressed were the heterogeneity of tumour size after implantation and the relatively rapid growth of the tumours which made the assessment of therapeutic effects challenging. Cells were checked by trypan blue exclusion prior to implantation to ensure adequate viability after harvest.

To improve consistency of analysis, each animal had its tumour injected when they had reached a pre-determined size of 3 to 4 mm in diameter. This allowed for the best ability to ascertain whether in principle a therapeutic advantage could be seen with combined therapy. Thus measurements and treatments were staggered across the experimental groups.

In the optimized analysis, C57 black6 mice were injected subcutaneously with $5x10^5$ AE17 cells and tumours were injected with PBS or Adwt ($1x10^9$ pfu Adwt in 100µl PBS of final volume, 10 mice per group). 3 ip injections of 100µg FGK45 in 100µl of PBS or PBS were given over the next 6 days. No limiting toxicities have been seen and there is an indication that combined therapy is more efficacious (Fig.5-9). It was also apparent that there was a strong response to FGK45 alone, which was more than expected.

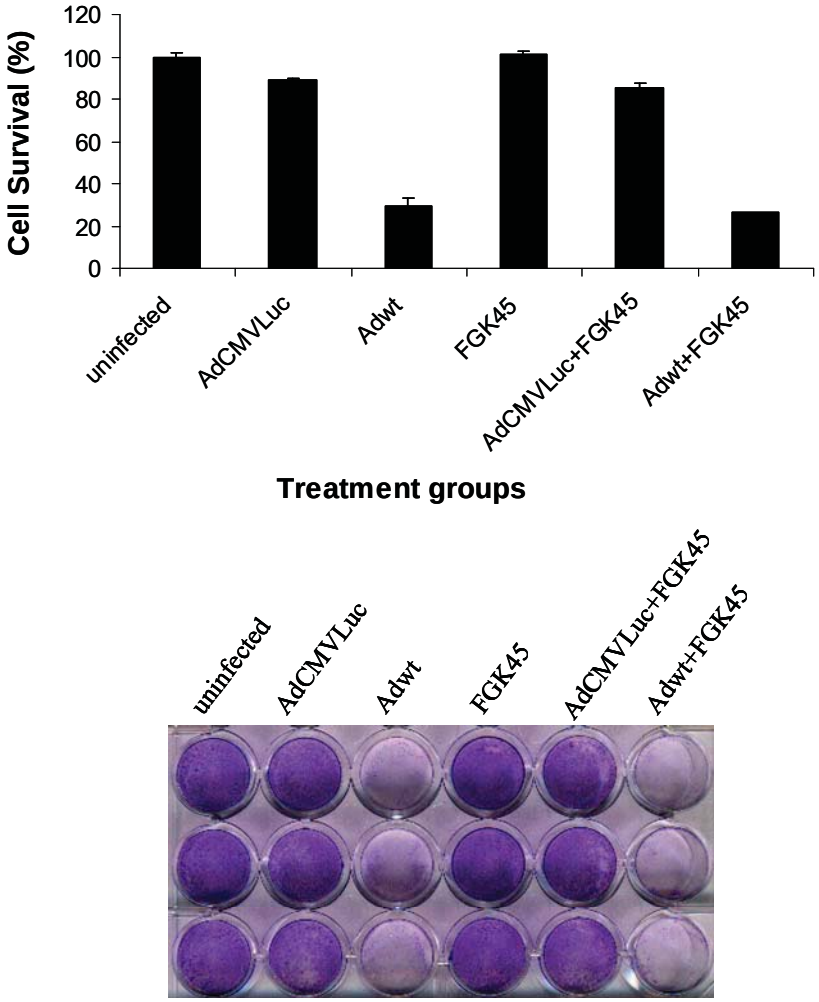

Fig. 5-8 Toxicity potency of FGK45 in AE17 mouse mesothelioma cells. AE17 cells were infected with: FGK45 alone, AdCMVLuc ± FGK45, Adwt ± FGK45 at pfu per cell of 100. The attached cells were stained with crystal violet 144 h post infection and cell viability was determined by measuring OD_{570nm}. Data was presented as the mean ± SD of triplicate wells.

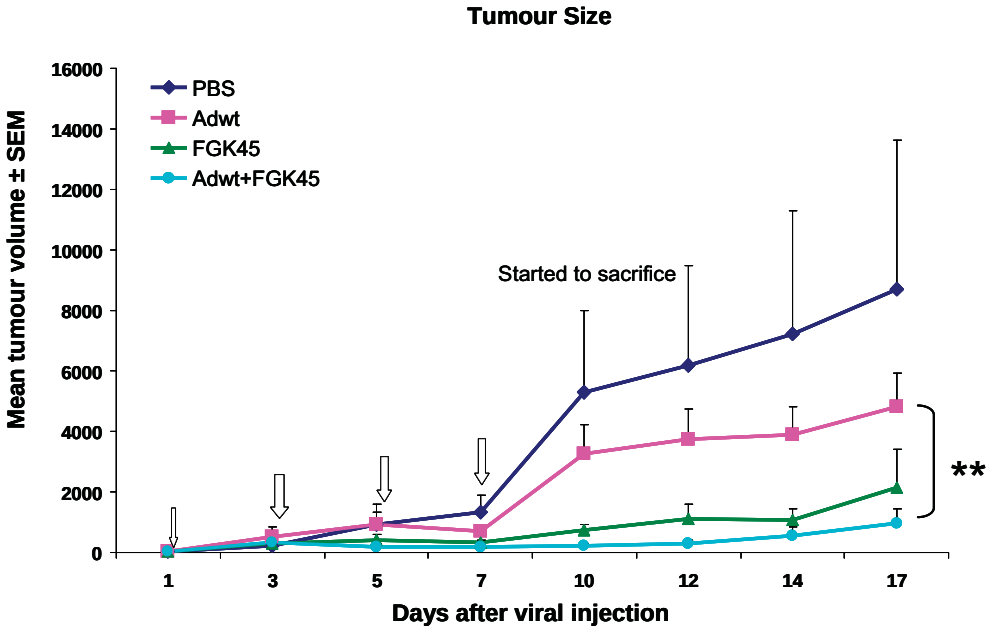

Fig. 5-9 Therapeutic effect of combination of Adwt and FGK45 *in vivo*. C57 black6 mice were injected subcutaneously with $5x10^5$ AE17 cells, and tumours were injected with PBS or Adwt. 3 ip injections of FGK45 were given over the next 6 days. After 10 days some mice had to be sacrificed- the size of the tumours at time of death has been carried forward in this analysis. Combination of Adwt and FGK45 significantly inhibited tumour growth. Data was presented as mean ± SEM. ** $p<0.01$ Adwt+FGK45 vs Adwt (n = 10 mice per group).

In further study, C57 black6 mice were injected subcutaneously with $5x10^5$ AE17 cells, and tumours were injected with PBS, AdCMVLuc or Adwt ($1x10^9$ pfu each virus in 100µl PBS of final volume, 10 mice per group). 3 ip injections of 100µg FGK45 in 100µl of PBS or PBS were given over the next 6 days (Fig.5-10). From 13 days onwards some mice had to be sacrificed- the size of the tumours at time of death has been carried forward in this analysis. The timing of sacrifice was made strictly in accordance with animal ethics guidelines and in consultation with animal facility staff. This assessment was made on the basis of the condition of the animal and a pre-determined upper limit of tumour size (total volume of tumour <20% of body weight).

I monitored tumour size and survival, and checked CD8+ T cell expression within the tumours by immunohistochemical staining (see 5.3.3.1). Fig.5-11 showed that FGK45 therapy significantly inhibited tumour growth. Combination of Adwt and FGK45 resulted in greater effect than Adwt or FGK45 alone. Although the combination of Adwt and FGK45 delayed the tumour growth compared to combination of control virus AdCMVLuc and FGK45, the effect is not significant. Significant differences were found in survival (Fig.5-12). All analyses were performed using SAS version 9.1 (Cary, NC, USA) by statisticians in the University of Adelaide. A poisson model was fitted to the data with group as the predictor variable with six categories – PBS, PBS +FGK45, AdCMVLuc, AdCMVLuc+FGK45, Adwt and Adwt+FGK45. The number of days to sacrifice was the response (count) variable. A P-value of less than 0.05 was required for statistical significance. P-values were adjusted for multiple comparisons using the stepdown sidak method. The count ratio describes the multiplication of the risk of an event (the 'risk' of being sacrificed in this case) that occurs with being in one group

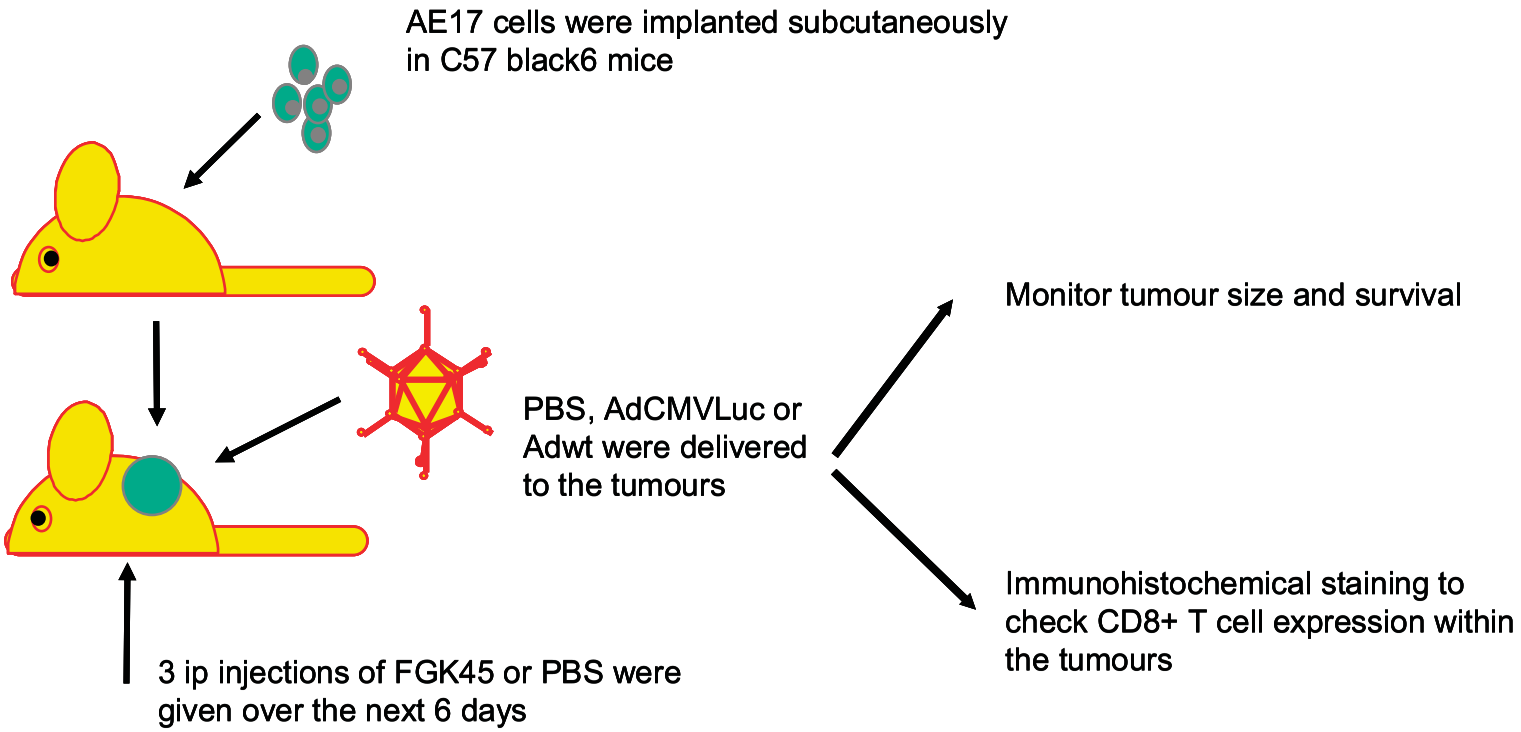

Fig. 5-10 Combined adenovirus and FGK45 in the immuno-competent murine mesothelioma model.

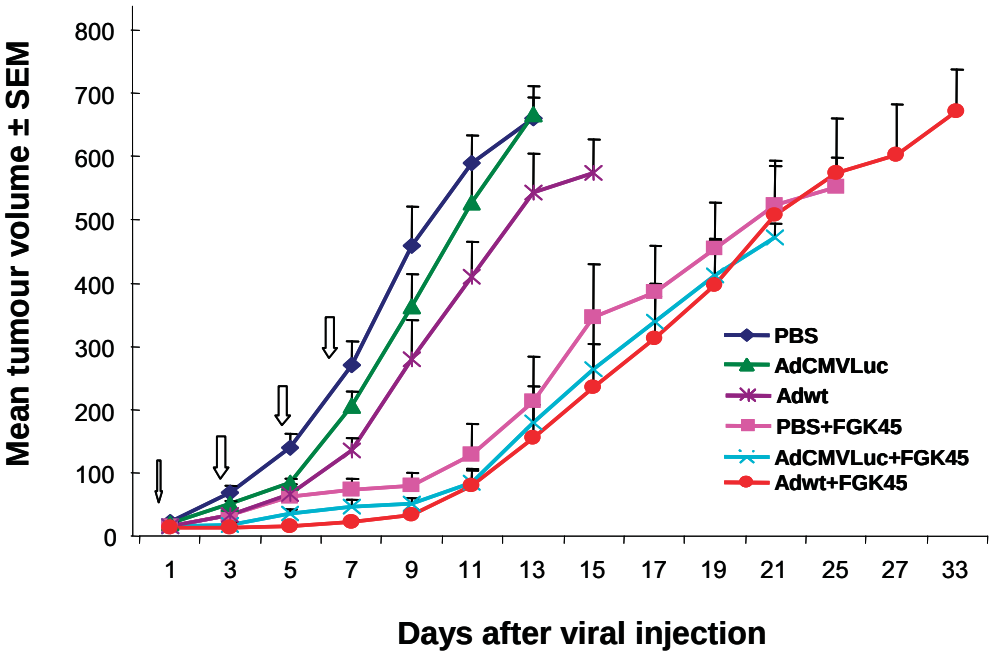

Fig. 5-11 Therapeutic effect of combination of Adwt and FGK45 *in vivo*. C57 black6 mice were injected subcutaneously with $5x10^5$ AE17 cells, and tumours were injected with PBS, AdCMVLuc or Adwt. 3 ip injections of FGK45 were given over the next 6 days. After 13 days some mice had to be sacrificed- the size of the tumours at time of death has been carried forward in this analysis. FGK45 significantly inhibited tumour growth. Combination of Adwt and FGK45 resulted in greatest growth inhibition. Data was presented as mean ± SEM. (n = 10 mice per group).

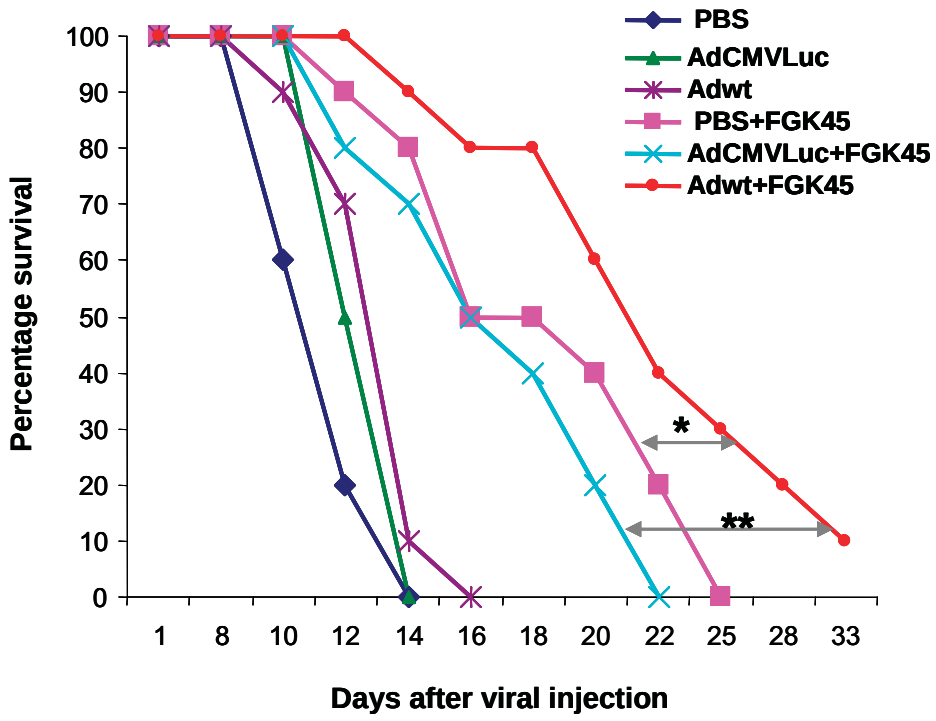

Fig. 5-12 Combination of Adwt and FGK45 resulted in greatest survival. C57 black6 mice were injected with AE17 tumours and treated with different groups as shown. Significant differences were found in the number of days to sacrifice between wt+FGK45 and PBS+FGK45 or Luc+FGK45. * $p < 0.05$ Adwt+FGK45 vs PBS+FGK45; ** $p<0.01$ Adwt+FGK45 vs Luc+FGK45.

compared to another group (for the categorical variable group). The estimated count ratio for days is 0.71 (p-value=0.038). This means that a mouse in group AdCMVLuc has 29% less days till sacrifice than a mice in AdCMVLuc+FGK45, which can be calculated by (1-0.71)*100 = 29. In other words, if a mouse is in group AdCMVLuc+FGK45 then they are likely to have more days till sacrifice than if they were in group AdCMVLuc. The 95% confidence interval for the count ratio is (0.56, 0.90). This means we can be 95% confident that the true count ratio in the population lies between 0.56 and 0.90. The other ratios and confidence intervals can be interpreted similarly. According to statistical analysis, combination of Adwt and FGK45 had 30% more days to sacrifice than combination of controls and FGK45.

5.3.4 Combination Therapy Augments T-cell Infiltration of the Tumour

5.3.4.1 Initial Analysis of Tumours from Therapy Study

In the analysis shown in 5.3.2, I found combination of Adwt and FGK45 resulted in greatest survival. T-cell infiltration of the tumours was analyzed at time of sacrifice by using immunohistochemistry. Immunohistochemical staining of CD8 T cells were performed on snap frozen tissues. CD8+ T cell expression could be detected in tumours treated with Adwt and all FGK45 combination groups (Fig.5-13). There are none or very fewer positive cells in the tumours treated with PBS or control virus groups. Combination of Adwt and FGK45 showed CD8+ T cell expression in more areas than other groups by manual counting.

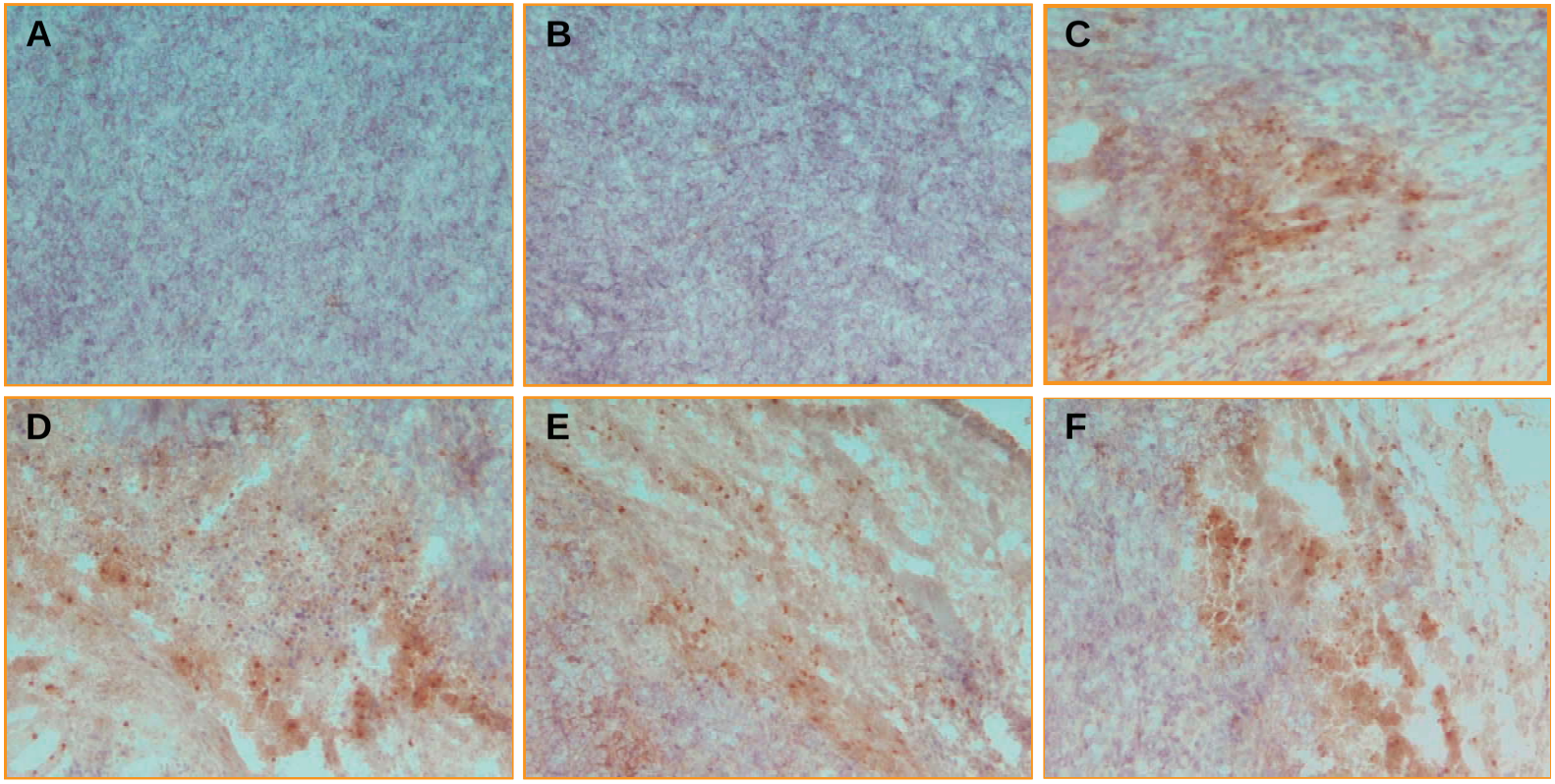

Fig. 5-13 CD8+ T-cell immunohistochemical staining in AE17 tumour at time of sacrifice. AE17 tumours were injected with 6 groups, A: PBS; B: AdCMVLuc; C: Adwt; D: PBS+FGK45; E: AdCMVLuc +FGK45; F: Adwt +FGK45. Immunohistochemical staining of CD8 T cells were performed on snap frozen tissues at time of death. CD8+ T cell expression of the tumours could be detected in tumours treated with Adwt and all FGK45 combination groups (x100 magnification).

5.3.4.2 Flow Cytometry Analysis of T-cell Infiltration

I already found that combination of Adwt and FGK45 showed CD8+ T cell expression in more areas than other groups. In order to quantify CD8 T cell expression, I performed another animal experiment. As described above, C57 black6 mice were injected subcutaneously with $5x10^5$ AE17 cells, and then tumours were injected with PBS, $1x10^9$ pfu of AdCMVLuc or Adwt (6 mice per group). 3 ip injections of FGK45 (100µg per injection) or PBS were given over the next 6 days. On Day 9 after treatment, all tumours were harvested. Tumour samples were disaggregated using a 'Medimachine' (BD Biosciences) for 2 min to prepare as a single cell suspension (Fig.5-14A). Effectiveness of the procedure was checked by staining a cytospin preparation of the disaggregated tissue with May Grunwald Giemsa (Fig.5-14B). CD8+ T cell expression in tumours was checked by flow cytometry on the same day. T-cells were initially gated based on positive staining with CD3 (Fig.5-15A), and the gated cells which were CD3 positive were further analyzed based on staining with CD8 (Fig.5-15B). Flow cytometry analysis of T-cell infiltration showed that CD8+ T cell expression was significantly increased in all FGK45 treated groups when compared to the without FGK45 treatment groups (Fig.5-16). Importantly, there was a marked increase in CD8+ T cell expression in the tumours treated with combination of Adwt and FGK45 compared with those of mice treated with combination of controls and FGK45.

A.

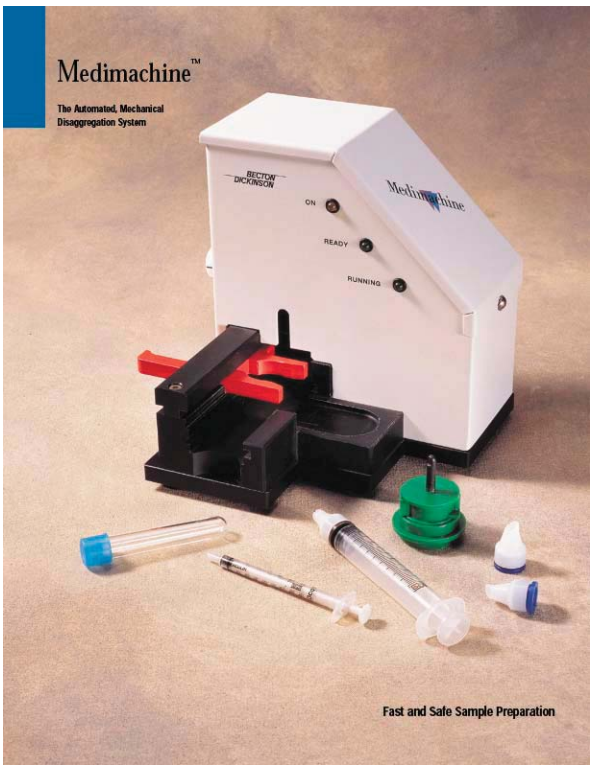

B.

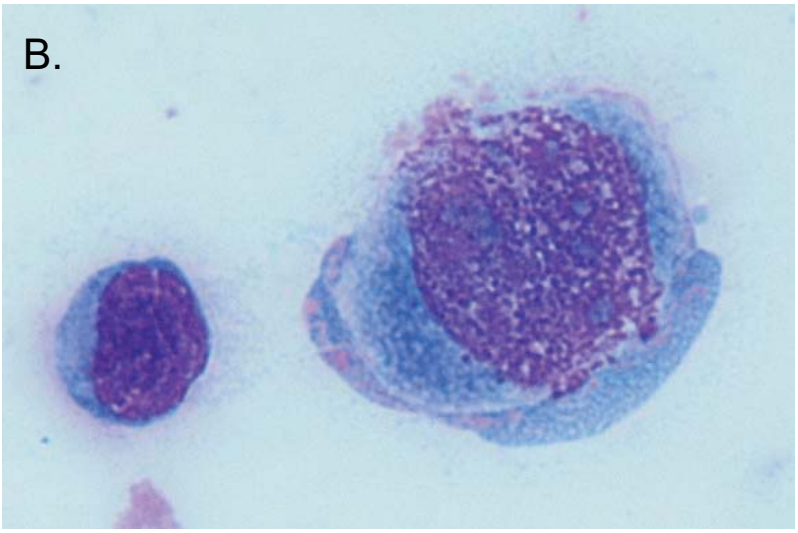

Fig. 5-14 Method of preparing a single cell suspension from solid tumour. A: Tumour samples were disaggregated using a 'Medimachine'(BD Biosciences) for 2 minutes; B: Effectiveness of the procedure was checked by staining a cytospin preparation of the disaggregated tissue with May Grunwald Giemsa.

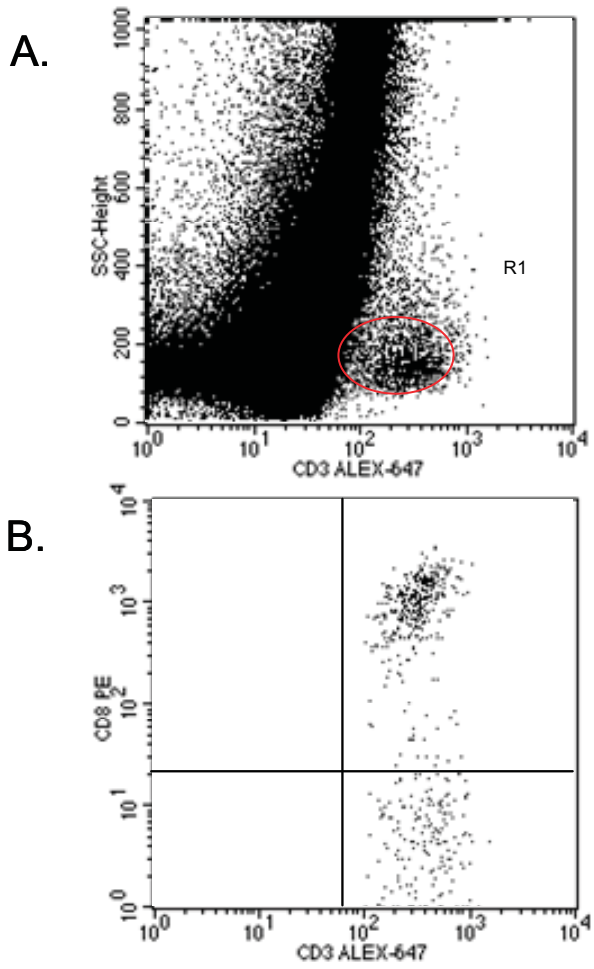

Fig. 5-15 Gating strategy for flow cytometric analysis of CD8+ T-cells.
A: T-cells were initially gated in Region 1 (R1) based on positive staining with CD3(conjugated to ALEXA-647); B: Cells from R1 were further analyzed based on staining with CD8 (conjugated to PE). Note 78% of cells showing staining characteristics consistent with CD8+ T-cells in the upper right quadrant.

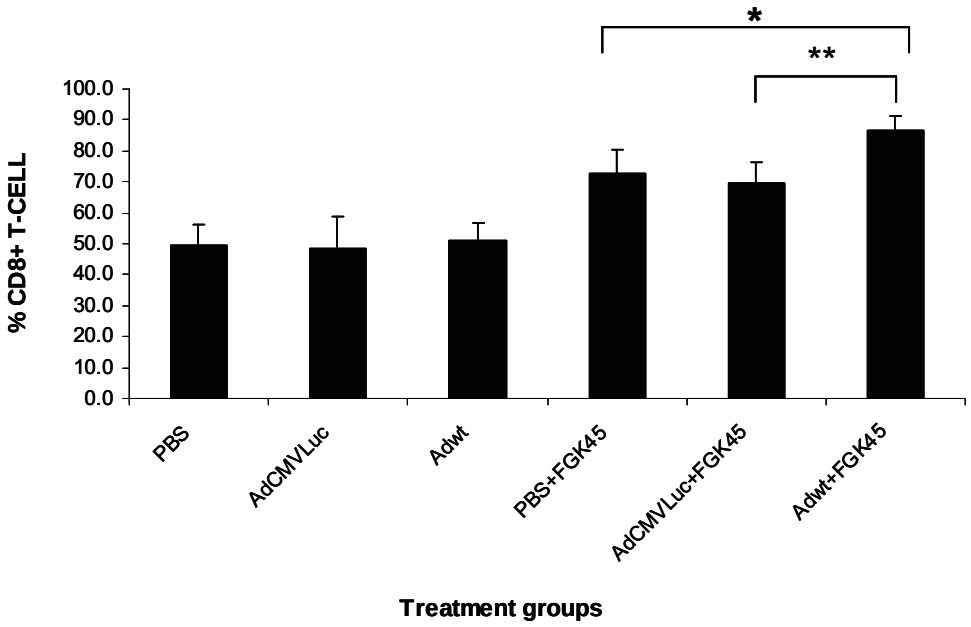

Fig. 5-16 Augmentation of CD8+ T-cell infiltration of tumours with combination therapy. Graph showed CD8 expression by AE17 tumour-associated T-cells. AE17 tumours were injected with: A: PBS; B: AdCMVLuc; C: Adwt; D: PBS+FGK45; E: AdCMVLuc +FGK45; F: Adwt +FGK45. The percentage of CD8+ T-cells was enumerated by flow cytometry 9 days following treatment. The mean values (± SD) are shown 6 mice per group (*P<0.05, ** P<0.001).

5.4 Discussion

Viral and immunotherapies have shown some limited efficacy in cancer treatment but neither has achieved impressive clinical results. A basic rationale exists to support that a combination of these approaches may improve outcomes.

I tested the cell-killing efficacy of wild type Ad and a CRAd (Δ24RGD) in a number of murine mesothelioma cells. Both Adwt and AdΔ24RGD demonstrated cell-killing and viral replicative capacity *in vitro*. In order to reduce the number of variables being assessed, only wild type Ad was chosen to evaluate the therapeutic efficacy *in vivo* the first instance. These studies focused on the wild type Ad alone or combined with FGK45, but established principles for CRAds in general and could be extended to AdΔ24RGD, VEGF or Flt-1 promoters controlling E1. Our ultimate aim is to evaluate the therapeutic efficacy of combined conditionally replicative adenovirus and tumour immuno-therapy in the immuno-competent murine model of mesothelioma and this is the subject of further studies.

Previous work (Nowak et al., 2003) confirmed the efficacy of the intraperitoneal FGK45 plus gemcitabine combination in the BALB/c mice model with a syngeneic AB1 cell line. Synergy between the drug and immunotherapy could be seen in the context of tumour cell death. However, FGK45 alone had minimal effect in the BALB/c mice model. In this study, I successfully established an adenovirus-susceptible, immuno-competent murine model (AE17) for mesothelioma, thus it is possible to determine the feasibility of combining replication competent viral therapy and immunotherapy. Using the AE17 model, I showed that FGK45 therapy significantly

inhibited tumour growth in the C57 black6 mice, in fact more than expected based on the published BALB/c results (Fig.5-10). This level of efficacy was very consistent across the studies performed. I hypothesised that the combination of Adwt and FGK45 would result in greatest tumour growth inhibition and better survival in the immuno-competent murine model of mesothelioma. The assessment of tumour size showed that the combination of Adwt and FGK45 delayed the tumour growth, but did not show a significant difference between Adwt and FGK45 versus control virus with FGK45. In terms of delaying time to death however, a small but significant advantage for wild type over control virus was noted. Further optimisation of the evaluation with respect to both virus and FGK45 dosing and duration is required. The model itself has some limitations in that once tumours are detectable they tend to grow very quickly. The size of tumours at time of death had been carried forward in this analysis. Some heterogeneity in tumour size was frequently noted and to overcome this I staggered therapy based on tumour size. FGK45 timing and dosing is another way to address the issue. Although previous work (Nowak et al., 2003) confirmed synergy between intraperitoneal FGK45 and gemcitabine combination in the BALB/c mice model, combined viral therapy with immunotherapy is still a new field. It is not known whether FGK45 would best be administrated concurrently or following Ad infection. I delivered FGK45 2 - 6 days after viral injection. Delivery of Adwt alone to AE17 tumours in the initial study delayed growth during 9 days after viral injection and the hypothesis was that this indicated viral toxicity and would be a rational time to assess immune-stimulation. During the period of treatment, FGK45 significantly inhibited tumour growth. However, rapid tumour growth occurred after the FGK45 delivery was stopped. In the current experiments duration of treatment was somewhat limited by the cost of the antibody,

but more prolonged therapy certainly appears worthy of investigation. Further refinements in dosing schedule and the use of CRAds are being pursued.

In this study, it has been shown that combination of Adwt and FGK45 resulted in greatest survival. I propose that this may be due to a greater influx of immune effector cells so I conducted additional experiments to quantify CD8 T cell expression in fresh tumours by flow cytometry. Tumours were harvested on Day 9 after treatment. There are some reasons why I chose to assess cellular responses 3 days after the completion of treatment. First, a previous study has reported that treatment with FGK45 alone causes a brief tumour regression over the treatment period, followed by rapid tumour outgrowth (Storniolo et al., 1997). Thus it appears that the antitumour effect of FGK45 may decrease shortly after treatment cessation (Nowak et al., 2003). Second, I found that delivery of Adwt alone to AE17 tumours causes a size reduction during 9 days after viral injection (Fig 5-6). Third, the graph of tumour size showed that combination of Adwt and FGK45 inhibited the tumour growth over 9 days of treatment, and rapid tumour growth could be detected after the treatment was ceased (Fig 5-10). On balance, my data confirms a greater influx on CD8+ cells with FGK45 treatment, which was further enhanced with replication viral therapy.

In conclusion the AE17 model may prove a useful platform for the investigation of further combinations of viral and immunotherapy. That having been said, the system is not ideal, and the level of viral replication seen in this model is less than I saw in a permissive human line. Nevertheless, in principle, the combination of viral and immunotherapy does appear more efficacious than either treatment alone, although the

benefits I have so far seen have been rather modest. Hopefully with further optimisation this combination will lead to a strategy that will have clinical benefits in future.